Lawrence Berkeley National Laboratory
LBL Publications

Title
A [CoSiH2] Silylene Synthon Provides Modular Access to Homo- and Heterobimetallic [Co═Si═M] (M = Co, Fe) Silicide Complexes.

Permalink
https://escholarship.org/uc/item/9jn938hw

Journal
Journal of the American Chemical Society, 145(45)

Authors
Handford, Rex
Tilley, Don

Publication Date
2023-10-31

DOI
10.1021/jacs.3c07998

Copyright Information
This work is made available under the terms of a Creative Commons Attribution License, available at https://creativecommons.org/licenses/by/4.0/

Peer reviewed

eScholarship.org Powered by the California Digital Library
University of California

JACS
JOURNAL OF THE AMERICAN CHEMICAL SOCIETY
pubs.acs.org/JACS
Article
Open Access
This article is licensed under CC-BY 4.0

A [$CoSiH_2$] Silylene Synthon Provides Modular Access to Homo- and Heterobimetallic [Co═Si═M] (M = Co, Fe) Silicide Complexes

Rex C. Handford and T. Don Tilley*

Cite This: *J. Am. Chem. Soc.* 2023, 145, 24690−24697
Read Online

ACCESS | Metrics & More | Article Recommendations | Supporting Information

ABSTRACT: Base-stabilized [BP_3^{iPr}](H)$_2$CoSiH$_2$(DMAP) (**1**, [BP_3^{iPr}] = PhB($CH_2P^iPr_2$)$_3^-$; DMAP = 4-dimethylaminopyridine) is a rare instance of a synthon for the simplest "parent" silylene complex (LM═SiH_2). Complex **1** was accessed in high yields via double Si−H bond activation in SiH_4 by [BP_3^{iPr}]Co(DMAP), and in solution, it undergoes rapid exchange between bound and free DMAP by an associative mechanism (as determined by variable-temperature ^{1}H NMR dynamic studies). The DMAP ligand of **1** is readily displaced by metal-based fragments that bind silicon and cleave the Si−H bonds of the SiH_2 moiety to produce bimetallic [Co═Si═M] (M = Co, Fe) molecular silicides. Thus, treatment of **1** with 0.5 equiv of (LCo^I)$_2$(μ-N$_2$) (L = a tripodal ligand) resulted in the spontaneous formation of [BP_3^{iPr}](H)$_2$Co═Si═Co(H)$_2$L (L = [BP_2^{tBu}Pz], PhB($CH_2P^tBu_2$)$_2$(pyrazolyl)$^-$ (**3**); Tp″, HB(3,5-diisopropylpyrazolyl)$_3^-$ (**4**)) with the concomitant release of DMAP. The symmetrical silicide [BP_3^{iPr}](H)$_2$Co═Si═Co(H)$_2$[BP_3^{iPr}] (**5**) was prepared by treatment of a mixture of **1** and [BP_3^{iPr}]Co(DMAP) with 2 equiv of Ph_3B, which in this case is required to sequester DMAP as the elimination product Ph_3B-DMAP. A heterobimetallic silicide, [BP_3^{iPr}](H)$_2$Co═Si═Fe(H)$_2$[SiP_3^{iPr}] (**7**; [SiP_3^{iPr}] = PhSi($CH_2P^iPr_2$)$_3$), was obtained via *in situ* KC_8 reduction of [SiP_3^{iPr}]FeCl and subsequent addition of **1** and Ph_3B. These transformations involving a metal−SiH_2 derivative demonstrate a fundamentally new type of reactivity for silylene complexes and provide a unique synthetic method for construction of molecular silicide complexes.

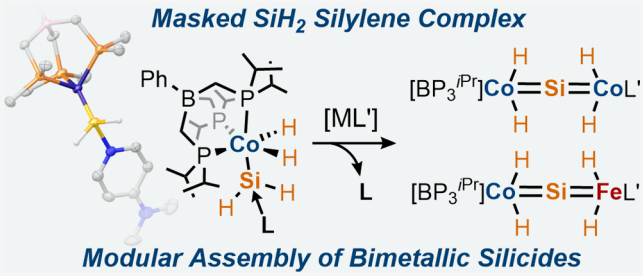

1. INTRODUCTION

Transition-metal−silicon materials are of broad importance to industry, catalysis, and solid-state technologies.[1−6] This is especially apparent in the direct process, which is responsible for the global production of chlorosilanes that serve as precursors to the silicone industry.[1,2] In this process, a copper catalyst combines with silicon to form copper silicide phases (e.g., Cu_3Si, Cu_5Si), and reactions with MeCl on the silicide surface produce silylene species [Cu_nSiClMe] that undergo further reaction to release Me_2SiCl_2 (Figure 1a).[1,2,7−11] Silicide phases find additional utility in the production of silicon nanomaterials (e.g., nanowires) using silanes as a source of silicon atoms.[4] These applications of solid-state silicides highlight the utility of both silicide (M_xSi_y) and silylene (LM═SiRR') reaction centers in promoting useful transformations, and a better understanding of both types of intermediates is expected to enable new silicon-based transformations. The latter challenge can be addressed with the study of well-defined molecular models designed to reveal mechanistic details and provide starting points for catalyst design strategies.[12−15]

Molecular silicide complexes are uncommon since there are very few general, controlled synthetic routes to molecules possessing M_xSi_y cores. Thus, an understanding of structure−function relationships for silicon atoms ligated to transition metals is severely lacking. Bimetallic silicides, LM═Si═ML,

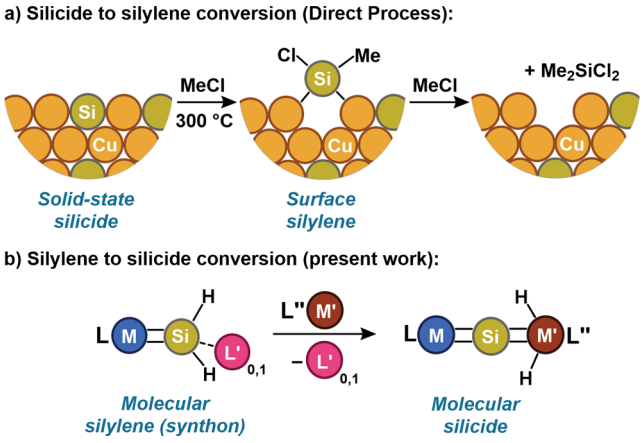

Figure 1. (a) Direct process reaction of copper silicide with MeCl to produce Me_2SiCl_2 via a silylene intermediate. (b) Conversion of a molecular SiH_2 complex (or synthon) to a molecular silicide.

Received: July 25, 2023
Revised: October 4, 2023
Accepted: October 5, 2023
Published: October 31, 2023

ACS Publications
© 2023 The Authors. Published by American Chemical Society

https://doi.org/10.1021/jacs.3c07998
J. Am. Chem. Soc. 2023, 145, 24690−24697

represent prototypical molecules of this class due to their structural simplicity and the high reactivity expected for the two-coordinate μ-silicon center. Access to such complexes was demonstrated through two primary strategies. In one case, metathetical exchange between (SIPr)$SiBr_2$ (SIPr = 1,3-*bis*-(2,6-diisopropylphenyl)-4,5-dihydroimidazol-2-ylidene) and 2 equiv of $[Tp^*Mo(CO)_2(PMe_3)]^-$ (Tp^* = HB(3,5-dimethylpyrazolyl)$_3^-$) produced the unsymmetrical silicide $Tp^*(OC)_2Mo{\equiv}Si{-}Mo(CO)_2(PMe_3)Tp^*$.[16] In addition, our laboratories reported the formation of [M═Si═M] cores from simple silanes, for example via quadruple Si−H bond activations of SiH_4 by $([BP_2^{tBu}Pz]Co)_2(\mu\text{-}N_2)$, to form $[BP_2^{tBu}Pz](H)_2Co{=}Si{=}Co(H)_2[BP_2^{tBu}Pz]$ ($[BP_2^{tBu}Pz]$ = $PhB(CH_2P^tBu_2)_2$(pyrazolyl)$^-$).[17] The [MSiM] cores of these silicides react in unprecedented ways; for example, the μ-silicon center of $Tp^*(OC)_2Mo{\equiv}Si{-}Mo(CO)_2(PMe_3)Tp^*$ binds alkynes to generate adducts incorporating planar, tetracoordinate silicon in $[(RCCR')SiMo_2]$ units.[18] In addition, reaction of $[BP_2^{tBu}Pz](H)_2Co{=}Si{=}Co(H)_2[BP_2^{tBu}Pz]$ with MeCl produced small quantities of functionalized silane products Me_xSiH_{4-x} (x = 1−3).[17]

Despite these recent advances, molecular silicide chemistry remains largely unexplored, mainly due to the absence of synthetic methods that provide control over stoichiometry and structural features (e.g., symmetry, coordination numbers, metal identities, etc.). The results reported here demonstrate the versatile, modular assembly of complex silicide structures by way of a synthon for the simplest terminal silylene complex, the adduct $[BP_3^{iPr}](H)_2CoSiH_2(DMAP)$ (**1**; $[BP_3^{iPr}]$ = $PhB(CH_2P^iPr_2)_3^-$; DMAP = 4-dimethylaminopyridine). This complex undergoes oxidative addition of the Si···H bonds by a second metal center to afford bimetallic complexes possessing a linear [MSiM′] core (Figure 1b).

2. RESULTS AND DISCUSSION

2.1. Access to a Base-Stabilized SiH_2 Complex. The base-stabilized silylene complex $[BP_3^{iPr}](H)_2CoSiH_2(DMAP)$ (**1**) was obtained by reaction of $[BP_3^{iPr}]Co(DMAP)$[19] with SiH_4 (1 equiv, 15% in nitrogen) in toluene (Scheme 1a), which

Scheme 1. (a) Synthesis of 1. (b) Solid-State Molecular Structure of 1 with 50% Probability Thermal Ellipsoids Drawn. Most Hydrogen Atoms Are Omitted for Clarity

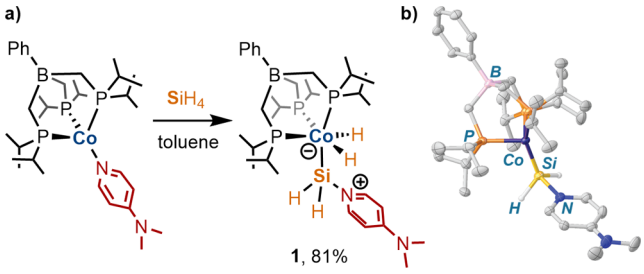

resulted in a color change from dark brown to bright orange. Complex **1** was isolated in high yield as an analytically pure solid following crystallization by diffusion of pentane into a saturated 1,2-difluorobenzene solution at −35 °C. The solid-state molecular structure of **1** consists of two unique molecules in the asymmetric unit, one of which exhibits considerable disorder of the $[BP_3^{iPr}]$ ligand; the structure of the non-disordered complex is shown in Scheme 1b. The Co−Si bond length in this molecule (2.135(2) Å) is modestly contracted in comparison to related base-stabilized cobalt silylenes (e.g., $[BP_3^{iPr}](H)_2CoSiHPh(DMAP)$, d(Co−Si) = 2.1524(8) Å;[19] $[BP_2^{tBu}Pz](H)_2CoSiHPh(DMAP)$, d(Co−Si) = 2.1428(5) Å[17]), reflecting a lower steric demand of the SiH_2(DMAP) "silylene" unit. Complex **1** appears to be only the second example of a $LMSiH_2(L')$ complex, since Radius et al. reported that reaction of *trans*-$Mes_2(Me_2Im)_2Fe$ with 2 equiv of $PhSiH_3$ produced $(Me_2Im)_2Fe[SiH_2(Me_2Im)][\mu\text{-}(H)_3SiHPh_2]$ via $PhSiH_3$ redistribution (Me_2Im = 1,3-dimethylimidazol-2-ylidene).[20]

In a benzene-d_6 solution, **1** exhibits dynamic behavior as evidenced by its ^1H and $^{31}P\{^1H\}$ NMR spectra. At 292 K, the Co−*H* and Si−*H* hydrogen nuclei resonate at δ −15.44 ppm (br s, 2H) and 6.36 ppm (*pseudo*-q, J = 7.5 Hz, $^1J_{SiH}$ = 159 Hz, 2H), respectively. The $^{31}P\{^1H\}$ NMR spectrum displays a single broad resonance at δ 62.6 ppm, indicating interconversion of phosphorus environments in the $[BP_3^{iPr}]$ ligand. The silicon nucleus of **1** resonates at δ 33 ppm according to a $^{29}Si{-}^1H$ HMBC NMR spectrum. Variable-temperature (VT) NMR spectroscopic studies of **1** in a toluene-d_8 solution show that upon cooling, the $^{31}P\{^1H\}$ NMR resonance decoalesces, and at 237 K, it is fully resolved into two resonances (1:2 ratio) at δ 61.1 and 62.9 ppm. The solution ^{29}Si chemical shift of complex **1**, coupled with the tetrahedral coordination geometry of silicon in the solid-state structure, indicates that there is minimal double-bond character within the Co−Si linkage, a feature that is consistent with other base-stabilized silylene species.[13]

The lability of the coordinated DMAP donor in **1** was of interest as an indication of possible reactivity modes for the SiH_2(DMAP) ligand. For context, note that previous VT-NMR studies of the base-stabilized silylene complex $[Cp^*(Me_3P)_2RuSiPh_2(NCMe)]^+$ (Cp^* = η^5-C_5Me_5) demonstrated that exchange of bound and free NCMe occurs by a dissociative mechanism involving a base-free $[Ru{=}SiPh_2]$ silylene intermediate.[21] Indeed, the ^1H NMR spectrum of a mixture containing **1** and 1 equiv of added DMAP (292 K, toluene-d_8) contains broadened resonances for the uncoordinated DMAP ligand, indicating a facile exchange process. Upon cooling, the resonances corresponding to coordinated and "free" DMAP sharpen. Line-shape analyses of spectra from 215 to 256 K provided an Eyring plot, from which $\Delta H^{\ddagger}$ (1.8 ± 0.2 kcal^{-1} mol^{-1}) and $\Delta S^{\ddagger}$ (−40.0 ± 0.7 J mol^{-1} K^{-1}) parameters were extracted ($\Delta G_{(298\ K)}^{\ddagger}$ = 13.7 ± 0.3 kcal^{-1} mol^{-1}). The large negative entropy of activation points to an associative mechanism for DMAP exchange in **1**, in contrast to the dissociative mechanism identified for $[Cp^*(Me_3P)_2RuSiPh_2(NCMe)]^+$.

A reasonable pathway for DMAP exchange in **1** involves the hypercoordinate intermediate $[BP_3^{iPr}](H)_2CoSiH_2(DMAP)_2$ (Scheme 2a). This exchange pathway was investigated by density functional theory (DFT) studies (ωB97X-D3/def2-TZVP(Co,Si,P),def2-SVP(C,H,B)// CPCM(toluene)) for the model complex $[BP_3^{Me}](H)_2CoSiH_2(DMAP)$ ($[BP_3^{Me}]$ = $PhB(CH_2PMe_2)_3^-$; **1***). The geometry-optimized structure of **1*** was obtained following the adaptation of the crystallographic atomic coordinates of **1**. A potential energy scan of rotation about the Co−Si bond identified a rotamer, **1*'** (Scheme 2b), which is further stabilized by −1.1 kcal^{-1} mol^{-1} compared to **1***; the rotamers **1*** and **1*'** are separated by a small rotational barrier of 5.0 kcal^{-1} mol^{-1} (Table S4). Exchange of DMAP with either **1*** or **1*'** is expected to involve the *bis*-DMAP adduct $[BP_3^{Me}](H)_2CoSiH_2(DMAP)_2$ (**Int**). A

https://doi.org/10.1021/jacs.3c07998
J. Am. Chem. Soc. 2023, 145, 24690−24697

Scheme 2. (a) Proposed Exchange Pathway for the DMAP Ligand of 1. (b) Reaction Coordinate Diagram for the DFT-Computed DMAP Exchange Mechanism of 1*'. The Stereochemistry of 1*' Is as Presented in the Scheme

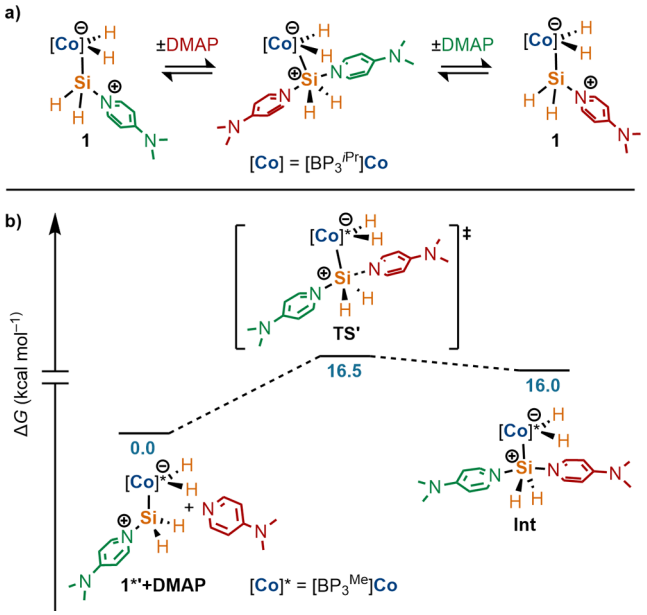

nudged-elastic band transition-state (NEB-TS)[22] search located transition-state structures for DMAP addition to **1*** or **1*'** to form **Int** (Scheme 2b). The calculated thermochemical parameters (relative to **1*'** + DMAP = 0 $kcal^{-1}$ mol^{-1}) of $\Delta H^{\ddagger}$ (4.4 $kcal^{-1}$ mol^{-1}), $\Delta S^{\ddagger}$ (−48.8 J mol^{-1} K^{-1}), and $\Delta G_{(298\ K)}{}^{\ddagger}$ (16.5 $kcal^{-1}$ mol^{-1}) are consistent with those derived from the Eyring plot, lending support to the proposed associative mechanism.

To examine whether DMAP could be removed from **1** by chemical abstraction, the complex was treated with 1 equiv of Ph_3B in a toluene solution. A darkening of the solution's color was immediately apparent, and ^1H and $^{31}P\{^1H\}$ NMR spectra of the reaction mixture indicated clean conversion to Ph_3B−DMAP and a new diamagnetic species, which was identified by X-ray crystallography and solution-state multinuclear NMR spectroscopy as $[PhB(CH_2P^iPr_2)_2](H)_2Co[\kappa^2\text{-}Si,P\text{-}H_2SiCH_2P^iPr_2]$ (**2**; Scheme 3). Complex **2** results from coupling of a $[BP_3{}^{iPr}]$ ligand $-CH_2P^iPr_2$ side arm with the SiH_2 moiety, suggesting the possible intermediacy of the base-free species $[BP_3{}^{iPr}](H)_2CoSiH_2$. However, the rapid course of the reaction (complete in <5 min) indicates that any such base-free silylene cannot be readily isolated under these conditions. Nevertheless, addition of Ph_3B to **1** represents a potential strategy for activating the $[SiH_2]$ unit toward further reactivity in the presence of a suitable substrate (*vide infra*).

Scheme 3. (a) Synthesis of 2. (b) Solid-State Molecular Structure of 2 with 50% Probability Thermal Ellipsoids. Most Hydrogen Atoms Are Omitted for Clarity

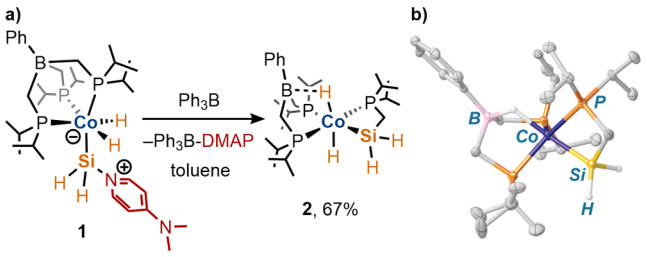

2.2. Homo- and Heterobimetallic Silicides. Possible transformations of $LMSiH_2$ and $LMSiH_2(L')$ species involve further activation of the Si−H bonds by an exogenous metal reagent to afford silicide complexes with a [MSiM′] core. Since donor-free $[BP_3{}^{iPr}](H)_2CoSiH_2$ has proven synthetically elusive, complex **1** was employed as a synthon in reactions with a second metal center designed to promote Si−H bond activation, DMAP displacement, and Si−M′ bond formations. As described below, this approach has led to the formation of bimetallic silicide complexes $[BP_3{}^{iPr}](H)_2Co{=}Si{=}M'(H)_2L$ (M′ = Co, Fe; L = tripodal ligand).

Previous work from this laboratory demonstrated that $([BP_2{}^{tBu}Pz]Co)_2(\mu\text{-}N_2)$ serves as a source of $[BP_2{}^{tBu}Pz]Co^I$, which readily activates the Si−H bonds of SiH_4 to generate the silicide $[BP_2{}^{tBu}Pz](H)_2Co{=}Si{=}Co(H)_2[BP_2{}^{tBu}Pz]$.[17] It therefore seemed that $([BP_2{}^{tBu}Pz]Co)_2(\mu\text{-}N_2)$, serving as a source of $[BP_2{}^{tBu}Pz]Co^I$, might react with **1** to generate the unsymmetrical silicide $[BP_3{}^{iPr}](H)_2Co{=}Si{=}Co(H)_2[BP_2{}^{tBu}Pz]$ (**3**). Indeed, the addition of a clear red-brown toluene solution of $([BP_2{}^{tBu}Pz]Co)_2(\mu\text{-}N_2)$ to a toluene solution of **1** resulted in a rapid color change to deep blue. Multinuclear ^1H and $^{31}P\{^1H\}$ NMR spectroscopic analyses of the crude reaction mixture indicated full consumption of the starting materials to form a new diamagnetic species whose features are consistent with **3**, in high (93%) yield, according to integration against an internal standard of $(Me_3Si)_2O$ (Scheme 4). Introduction of

Scheme 4. (a) Reaction of 1 with $(LCo)_2(\mu\text{-}N_2)$ to Form Silicides 3 and 4 (L = $[BP_2{}^{tBu}Pz]$, Tp″). Spontaneously Released DMAP Is Sequestered by Ph_3B. (b) Depiction of Molecular Structures of 3 and 4

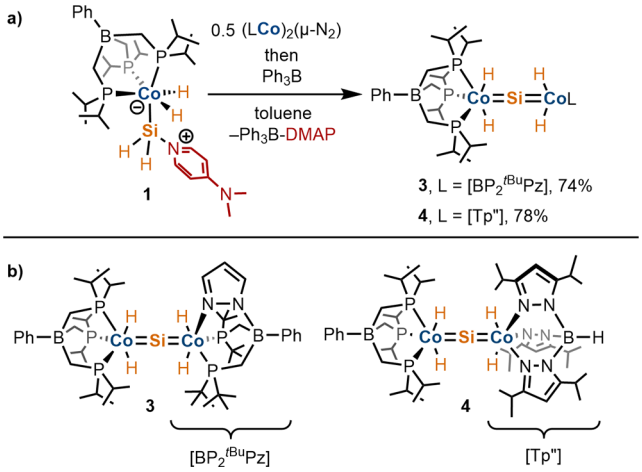

Ph_3B to the reaction mixture resulted in near-quantitative capture of the released DMAP to form Ph_3B−DMAP (97%, via ^1H NMR spectroscopy). The adduct Ph_3B−DMAP was conveniently removed from the reaction mixture via crystallization by diffusion of pentane into a dilute tetrahydrofuran (THF) solution at −35 °C. Complex **3**, enriched in the supernatant solution, was crystallized by diffusion of $(Me_3Si)_2O$ into a saturated THF solution cooled to −35 °C and was isolated in an analytically pure form in good yield (74%).

https://doi.org/10.1021/jacs.3c07998
J. Am. Chem. Soc. 2023, 145, 24690−24697

An additional unsymmetrical dicobalt silicide, $[BP_3^{iPr}]$-$(H)_2Co{=}Si{=}Co(H)_2Tp''$ (**4**, Tp″ = HB(3,5-diisopropylpyrazolyl)$_3^-$), was generated in an analogous fashion by treatment of **1** with 0.5 equiv of $(Tp''Co)_2(\mu\text{-}N_2)$.[17] A color change of the reaction mixture from dark brown to blue was observed upon addition of $(Tp''Co)_2(\mu\text{-}N_2)$, and multinuclear NMR spectroscopy (^{1}H, ^{31}P{^{1}H}) indicated formation of a single diamagnetic species (in addition to DMAP) possessing features consistent with $[BP_3^{iPr}](H)_2Co{=}Si{=}Co(H)_2Tp''$ (**4**; Scheme 4). Complex **4** was isolated as an analytically pure dark-blue powder, following precipitation from a concentrated diethyl ether solution. However, **4** has yet to be isolated in a crystalline form suitable for X-ray diffraction studies.

The isolation of **4** is surprising as direct treatment of $(Tp''Co)_2(\mu\text{-}N_2)$ with SiH_4 or $PhSiH_3$ has been shown to result in mixtures of the μ-hydrides $(Tp''Co)_2(\mu\text{-}H)_x$ (x = 1, 2).[17] This hydrogen-atom abstraction was favored over silicide formation, possibly due to the inability of the Tp″ ligands to enforce sufficiently long Co···Co separations to stabilize a linear [CoSiCo] core.[17] Thus, the accessibility of **4** is likely related to beneficial steric properties for the $[BP_3^{iPr}]$ ligand.

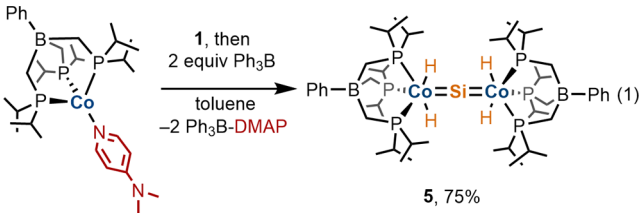

Using this synthetic approach, complex **1** was converted to the symmetrical homobimetallic silicide $[BP_3^{iPr}](H)_2Co{=}Si{=}Co(H)_2[BP_3^{iPr}]$ (**5**; eq 1). Complex **5** has remained elusive despite previous attempts to access this structure by treatment of $Na(THF)_6([BP_3^{iPr}]CoI)$ with 0.5 equiv of SiH_4.[19] In that case, the silicide $[BP_3^{iPr}](H)_2Co{=}Si{=}Co(H)_2(SiH_3)$-$[(^iPr_2PCH_2)_2BPh]$ was generated via a process involving the degradation of a $[BP_3^{iPr}]$ ligand. With complex **1** in hand, **5** was synthesized by addition of 2 equiv of Ph_3B to a solution containing **1** and $[BP_3^{iPr}]Co(DMAP)$ (eq 1). Monitoring the reaction by ^{1}H NMR spectroscopy showed that prior to the addition of Ph_3B, no reaction of the starting complexes was evident. Addition of Ph_3B was accompanied by a rapid color change from dark orange-brown to red, and ^{1}H and ^{31}P{^{1}H} NMR spectroscopic analyses of the crude reaction mixture indicated that **5** and Ph_3B—DMAP were generated as the exclusive products in quantitative yields. Complex **5** was isolated as an analytically pure crystalline solid by crystallization from a concentrated neat THF solution.

In contrast to the reactions that produce **3** and **4**, the reaction of **1** and $[BP_3^{iPr}]Co(DMAP)$ to generate **5** did not spontaneously liberate DMAP. Thus, coordinatively labile starting materials are not strictly necessary for silicide formation, and Ph_3B is a potential trigger for such coupling processes. By analogy with the reactions depicted in Scheme 4, another potentially suitable starting material for the preparation of **5** seemed to be the μ-dinitrogen complex $([BP_3^{iPr}]$-$Co)_2(\mu\text{-}N_2)$ (**6**). Complex **6** was independently generated by the addition of Ph_3B to $[BP_3^{iPr}]Co(DMAP)$ in a benzene-d_6 solution in high yield (Scheme 5a). Complex **6** is thermally sensitive and decomposes to an intractable brown-colored material upon exposure to vacuum although small quantities of crystalline **6** were obtained following storage of a $(Me_3Si)_2O$/

Scheme 5. (a) *In Situ* Generation of 6 via DMAP Abstraction from $[BP_3^{iPr}]Co(DMAP)$. (b) Reaction of 6 with 1 to Generate a Mixture Containing $[BP_3^{iPr}]Co(DMAP)$, 1, and 5, and Subsequent Convergence of the Reaction Mixture to 5 upon Addition of Ph_3B. *Yield Determined by Integration of the ^{1}H NMR Spectrum against an Internal Standard

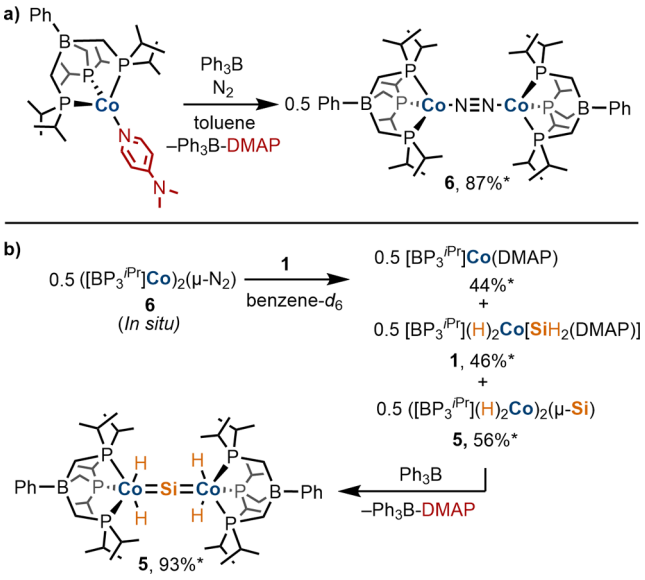

benzene-d_6 mixture at −35 °C, allowing for structural determination by single-crystal X-ray diffraction analysis (see the Supporting Information page S16).

Surprisingly, ^{1}H and ^{31}P{^{1}H} NMR spectroscopic monitoring of the reaction of *in situ* generated **6** (0.5 equiv) and **1** (1 equiv) revealed the formation of a mixture containing 0.5 equiv of $[BP_3^{iPr}]Co(DMAP)$, 0.5 equiv of **1**, and 0.5 equiv of **5** rather than full conversion to **5** (Scheme 5b). Further addition of Ph_3B (1 equiv) resulted in the near-quantitative formation of **5** and Ph_3B—DMAP (by integration of the ^{1}H NMR spectrum against an internal standard). These observations are consistent with a dynamic system in which **6** serves both to activate Si−H bonds in **1** and to abstract DMAP. The latter event results in sequestration of 0.5 equiv of $[BP_3^{iPr}]Co^I$ units supplied by **6** as $[BP_3^{iPr}]Co(DMAP)$, necessitating an additional equiv of Ph_3B for complete conversion to **5**. The differing behavior of **6** toward **1** in comparison to the congeneric $[BP_2^{tBu}Pz]$- and Tp″-complexes indicates that DMAP is the most strongly bound to the $[BP_3^{iPr}]Co^I$ fragment.

The utility of **1** for preparation of *hetero*bimetallic silicides (i.e., [MSiM′]) was also evaluated. For this purpose, the Fe^I starting material $[SiP_3^{iPr}]FeCl$ ($[SiP_3^{iPr}]$ = $PhSi(CH_2P^iPr_2)_3$), previously reported by this laboratory,[23] was employed. It seemed that the 14-electron $[SiP_3^{iPr}]Fe^0$ fragment, which is electronically similar to $[BP_3^{iPr}]Co^I$, would be well suited for activation of the Si−H bonds of **1**. Treatment of $[SiP_3^{iPr}]FeCl$ with 1 equiv of KC_8 in a THF solution was accompanied by a color change from clear green to dark red. Although the dark-red intermediate has yet to be characterized, closely related tridentate *tris*-phosphine iron(0) systems have been described and isolated as $LFe(N_2)_2$ adducts.[24,25] No conversion to a silicide was apparent upon addition of **1** to the dark-red solution, according to ^{1}H and ^{31}P{^{1}H} NMR spectroscopies. However, the addition of Ph_3B to the reaction mixture resulted in rapid conversion to a new diamagnetic species, formulated

https://doi.org/10.1021/jacs.3c07998
J. Am. Chem. Soc. 2023, 145, 24690−24697

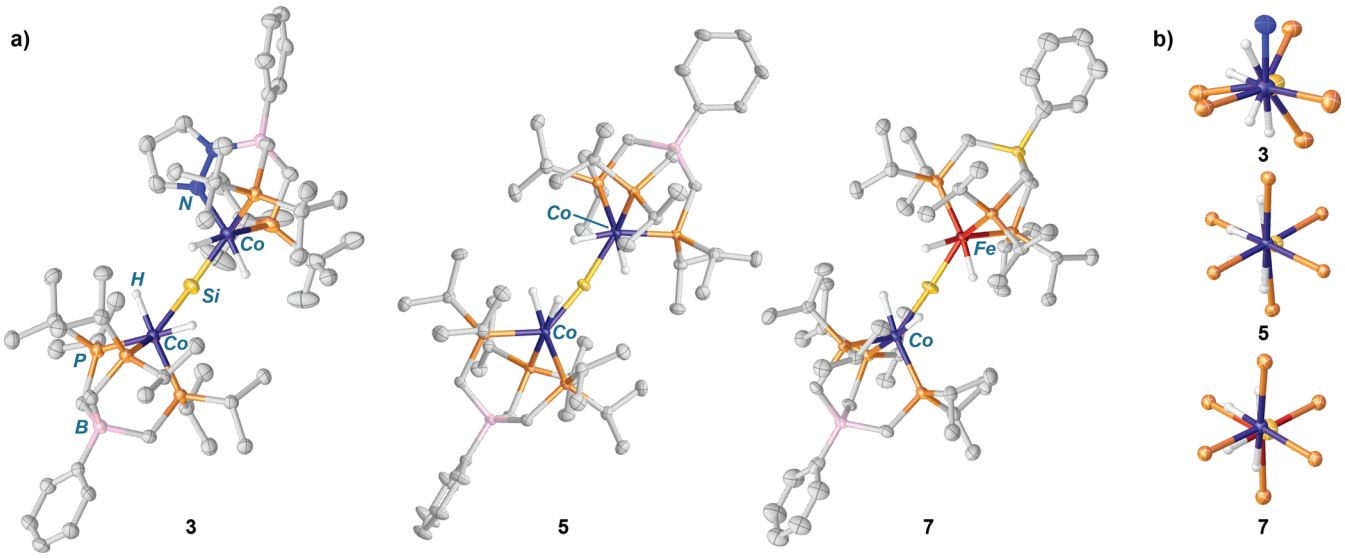

Figure 2. (a) Solid-sate molecular structures of silicide molecules **3**, **5**, and **7** with 50% probability thermal ellipsoids drawn. Most hydrogen atoms are omitted for clarity. (b) Views of **3**, **5**, and **7** along the Co···M′ (M′ = Co, Fe) axes, illustrating nontetrahedral arrays of hydride ligands about the μ-silicon atoms.

Table 1. Tabulated Experimental and Computed Metrical Parameters and Solution ^{29}Si NMR Data for Silicide Complexes 3, 4, 5, and 7

species	δ_{Si} (ppm)[a]	d(Co^A−Si)[b] (Å)	d(Si−M′)[b] (Å)	∠(Co−Si−M′) (degrees)	WBI (Co^A−Si)[b]	WBI (Si−M′)	qCo^A	qM′	qSi
3	305	2.086(2)	2.084(2)	169.00(5)					
3*		2.071	2.068	163.9	1.44	1.48	−0.30	0.00	+0.52
4	264								
5	333	2.0883(6)	2.0883(6)[c]	166.11(5)					
5[e]		2.071	2.070	163.0	1.44	1.44	−0.31	−0.31	+0.50
7	358, −5[d]	2.096(9)	2.096(9)[c]	169.0(4)					
7*		2.098	2.072	162.0	1.40	1.56	−0.34	−0.88	+0.53

[a]Recorded in benzene-d_6 solution (119 MHz). [b]Co^A is the [BP$_3^{iPr}$]-ligated cobalt atom; M′ refers to the second metal atom in each complex (Co or Fe). [c]Generated from symmetry equivalent fragments. [d]Recorded in THF-d_8 solution (119 MHz). [e]Asterisks denote DFT-computed molecules.

as [BP$_3^{iPr}$](H)$_2$Co═Si═Fe(H)$_2$[SiP$_3^{iPr}$] (**7**; eq 2). Complex **7** was authenticated by single-crystal X-ray diffraction analysis (Figure 2a, right), elemental analysis, and multinuclear NMR spectroscopy (*vide infra*).

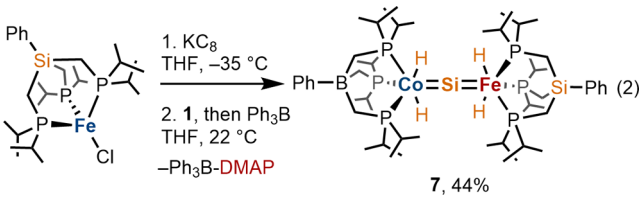

2.3. Spectroscopic and Structural Properties of Silicides. The ^{1}H, ^{31}P{^{1}H}, and ^{29}Si{^{1}H} DEPT NMR spectra of **3**, **4**, **5**, and **7** display features consistent with silicide structures of this class.[17,19] Owing to its high molecular symmetry, complex **5** displays the most straightforward NMR spectroscopic features. In benzene-d_6 solution, the hydride ligands of **5** appear as a broad singlet (δ −13.16 ppm, 4H) in the ^{1}H NMR spectrum, and only one line is displayed in the ^{31}P{^{1}H} NMR spectrum (δ 65.5 ppm). The NMR spectroscopic features of **3** resemble a superposition of those for **5** and [BP$_2^{tBu}$Pz](H)$_2$Co═Si═Co(H)$_2$[BP$_2^{tBu}$Pz], reflecting the incorporation of [BP$_3^{iPr}$](H)$_2$Co and [BP$_2^{tBu}$Pz](H)$_2$Co fragments into **3**.[17] The hydride resonances of **3** appear at δ −13.02 ppm ([BP$_3^{iPr}$](*H*)$_2$Co, 2H), −24.58 ppm ([BP$_2^{tBu}$Pz](*H*)$_2$Co, 1H), and −9.91 ppm ([BP$_2^{tBu}$Pz](*H*)$_2$Co, 1H). The "blended" character of **3** is also apparent in the ^{31}P{^{1}H} NMR spectrum, which displays resonances at δ 65.6 ppm ([BP$_3^{iPr}$]) and 78.8 ppm ([BP$_2^{tBu}$Pz]) in a ca. 3:2 ratio, respectively. For **4** and **7**, two distinct 2:2 resonances are apparent in the high-field ("hydride") regions of their ^{1}H NMR spectra. For **3**, **4**, and **5**, H−Si and H−P coupling were not observable for the hydride resonances, presumably due to the presence of quadrupolar ^{59}Co (I = 7/2) nuclei.[26] The heterobimetallic silicide **7** is unique in this regard as fine structure of the Fe−*H* resonance is present (δ −14.49 ppm, $^2J_{HP}$ = 16.9 Hz); notably, ^{29}Si satellites for this resonance were not detectable in either the ^{1}H or ^{1}H{^{31}P} NMR spectra of **7**, implying minimal coupling to the μ-silicon nucleus.

A notable feature of these silicides is the low-field ^{29}Si resonances in their ^{29}Si{^{1}H} DEPT NMR spectra (δ 264−358 ppm; Table 1). These ^{29}Si chemical shifts span a well-defined range that is diagnostic for this family of 3d-metal silicides and is consistent with structurally related, previously reported silicides.[17,19] Notably, the 4d- and 5d-metal silicides in the Tp*(OC)$_2$M≡Si−M(CO)$_2$(L)Tp* class (M = Mo, W) generally possess lower-field ^{29}Si resonances (δ 396−439).[16,18,27]

Comparison of the solid-state molecular structures of **3**, **5**, and **7** reveal similar geometries for the [(H)$_2$M═Si═M′(H)$_2$] cores (M = Co, M′ = Co, Fe). The metric parameters for the

https://doi.org/10.1021/jacs.3c07998
J. Am. Chem. Soc. 2023, 145, 24690−24697

solid-state structures are summarized in Table 1. In each case, the single-crystal X-ray diffraction data are of sufficient quality for location of the hydride ligands in the difference maps; accordingly, these hydrogen atoms were refined isotropically. For **3**, **5**, and **7**, the hydride ligands do not form a tetrahedral array about the μ-silicon atom, which would be expected for [M(μ-SiH_4)M′] systems in which Si−H activation is minimal.[28,29] Instead, the hydride ligands are oriented to accommodate a *pseudo*-octahedral coordination geometry for the associated metal centers (Figure 2b). Additionally, in **3**, **5**, and **7**, the hydride ligands of the neighboring [L(H)$_2$M] units are canted toward one hemisphere of the molecule, leaving a face of the μ-silicon atom exposed. These features are consistent across **3**, **5**, and **7**, as shown in Figure 2b, which presents perspective views of the silicide solid-state structures along the Co···M′ axes. Coupled with the solution-state multinuclear NMR data for these species, the data strongly point toward assignment of these silicides as [(H)$_2$M═Si═M′(H)$_2$] rather than [M(μ-SiH_4)M′] structures, in which significant residual Si···H interactions are present.[17,19,28,29]

The asymmetric unit in the crystal structure of **3** contains one nondisordered molecule of [BP_3^{iPr}](H)$_2$Co═Si═Co(H)$_2$[BP_2^{tBu}Pz], displaying close Co−Si contacts (d([BP_3^{iPr}]Co−Si) = 2.086(2) Å, d([BP_2^{tBu}Pz]Co−Si) = 2.084(2) Å), and a nearly linear Co−Si−Co linkage (∠= 169.00(5)°). For crystals of **5** and **7** grown from neat THF solutions at −35 °C, the asymmetric units of their crystal structures (in $C2/c$) contain half of a molecule; the full molecules are generated by a symmetry operation. For complex **7**, this feature of the solid-state molecular structure precludes the distinction of the M−Si bond lengths. The presence of a half-occupied silicon atom at the bridgehead site of the overlapping [BP_3^{iPr}]/[SiP_3^{iPr}] ligands is apparent from the electron density map, and the site is well-modeled as being occupied by 0.5 B and 0.5 Si atoms. Significant distortions of the atomic thermal parameters occurred when the site was modeled as either fully occupied boron or silicon.

Geometry optimizations (DFT) of **3**, **5**, and **7** were initiated from the crystallographic atomic coordinates at the ωB97X-D3/def2-TZVP(Co,Fe,Si,P),def2-SVP(C,H,B,N) level of theory. Across the series, the natural charge[30] (q) distribution in the [CoSiM′] cores of (nontruncated) **3***, **5***, and **7*** remains broadly consistent, with modest positive charge accumulation at the μ-silicon atom (Table 1). The small but generally slightly negative charges of the metal centers in **3***, **5***, and **7*** indicate that the metal centers are not well-described as Co^V and Fe^{IV} in the oxidation state formalism, which is often ambiguous in cases of atoms engaged in highly covalent bonding.[31,32]

Analysis of the Wiberg bond indices[33] (WBIs) of **3***, **5***, and **7*** provided further insight into the bonding situation within these molecules (Table 1). The magnitudes of the metal−silicon WBIs are similar to those previously reported for [BP_2^{tBu}Pz](H)$_2$Co═Si═Co(H)$_2$[BP_2^{tBu}Pz] (1.47, 1.47)[17] and [BP_3^{iPr}](H)$_2$Co═Si═Co(H)$_2$(SiH_2Ph)[($^iPr_2PCH_2$)$_2$BPh] (1.45, 1.44).[19] In heterobimetallic silicide **7**, the differing Co···Si and Fe···Si WBIs potentially indicate a greater extent of Fe···Si multiple bonding. This effect may be related to a greater donation from iron, which can be rationalized by considering isolated [BP_3^{iPr}]Co^I and [SiP_3^{iPr}]Fe^0 fragments. Also, the borate ligand of [BP_3^{iPr}]Co^I introduces a formal positive charge at the metal center for the overall neutral fragment, perhaps contracting the valence metal-based orbitals. In contrast, the neutral [SiP_3^{iPr}]Fe^0 fragment formally possesses a zerovalent metal center, which is expected to more effectively mediate the cleavage of Si−H bonds.

Atoms in molecules (AIM)[34] analyses of **3**, **5**, and **7** showed that the [H_2Co═Si═MH_2] (M = Fe, Co) cores in these silicides possess few or no bond paths/bond critical points connecting the μ-silicon centers and the flanking hydride ligands (Figure S21). One bond path connecting the hydride ligand oriented *cis* with respect to the N-donor atom of the [BP_2^{tBu}Pz] ligand of **3** to the μ-silicon center is present, analogous to the situation found in [BP_2^{tBu}Pz](H)$_2$Co═Si═Co(H)$_2$[BP_2^{tBu}Pz].[17] One such bond path is also present in **5**. These features may indicate a minor Si···H interaction;[19,35−38] similarly, in the case of [BP_3^{iPr}](H)$_2$Co═Si═Co(H)$_2$(SiH_2Ph)[($^iPr_2PCH_2$)$_2$BPh],[19] the value of $^1J_{Si-H}$ (8 Hz) was found to be consistent with minimal Si−H bonding.

3. CONCLUSIONS

Base-stabilized silylene (SiH_2) complex **1** has enabled facile, modular access to a series of symmetrical, unsymmetrical, and heterobimetallic silicides via Si···H bond activations. In certain cases, **1** allowed access to silicides that are not obtainable by direct L(H)$_2$M═Si═M(H)$_2$L formation from SiH_4 and a (LM)$_2$(μ-N_2) precursor. For example, reaction of (Tp″Co)$_2$(μ-N_2) with SiH_4 was found to generate mixtures containing (Tp″Co)$_2$(μ-H)$_{1,2}$ as opposed to a silicide product.[17] This result implies that the presence of a bulky [BP_3^{iPr}]Co unit stabilizes silicide structures that are inaccessible with other ligand combinations, as demonstrated by [BP_3^{iPr}]Co/Tp″Co silicide **4**, which is isolable. Similarly, the symmetrical silicide **5** is inaccessible by direct treatment of Na(THF)$_6$([BP_3^{iPr}]CoI) or **6** with SiH_4; in these cases, [BP_3^{iPr}](H)$_2$Co═Si═Co(H)$_2$(SiH_3)[($^iPr_2PCH_2$)$_2$BPh][19] or a mixture of **2** and **5** (both in ∼20% yield)[39] is produced as the major silicon-containing product, respectively. Thus, **1** avoids degradation pathways involving the [BP_3^{iPr}] ligand, such as −$CH_2P^iPr_2$ side-arm migration and coupling to generate [$H_2SiCH_2P^iPr_2$] fragments, as seen in **2**. This feature is likely derived from the base stabilization in **1**, which tempers the high reactivity expected for a base-free terminal SiH_2 complex.

The extension of silicide chemistry to heterobimetallic metal combinations, as in complex **7**, presents a new metal−silicon structural type and potentially new avenues for cooperative substrate activation and silicon atom functionalization that exploit diverse electronic properties of the metal centers. Significantly, precursor silylene complex **1** demonstrates a novel type of reactivity for transition-metal silylene complexes (i.e., metal-mediated Si−H bond activation of a coordinated silylene) and highlights the utility of [SiH_2] synthons for accessing unusual metal−silicon bonding arrangements.

■ ASSOCIATED CONTENT

Supporting Information

The Supporting Information is available free of charge at https://pubs.acs.org/doi/10.1021/jacs.3c07998.

Experimental methods, detailed syntheses, details of VT-NMR spectroscopy, details of crystallography, details of calculations, NMR spectra, computed atomic coordinates (PDF)

https://doi.org/10.1021/jacs.3c07998
J. Am. Chem. Soc. 2023, 145, 24690−24697

AUTHOR INFORMATION

Corresponding Author

T. Don Tilley − *Department of Chemistry, University of California, Berkeley, Berkeley, California 94720, United States;* orcid.org/0000-0002-6671-9099; Email: tdtilley@berkeley.edu

Author

Rex C. Handford − *Department of Chemistry, University of California, Berkeley, Berkeley, California 94720, United States;* orcid.org/0000-0002-3693-1697

Complete contact information is available at: https://pubs.acs.org/10.1021/jacs.3c07998

Notes

The authors declare no competing financial interest.

ACKNOWLEDGMENTS

This work was funded by the National Science Foundation under grant no. CHE-1954808. R.C.H. thanks the NSERC of Canada for a PGS-D fellowship. This research used the resources of the Advanced Light Source, which is a DOE Office of Science User Facility under contract no. DE-AC02-05CH11231. Computations were performed using the Tiger cluster at the Molecular Graphics and Computation Facility (MGCF) of the University of California, Berkeley, which is supported by the National Institutes of Health under grant no. NIH S10OD023532. The authors thank Dr. Kathleen Durkin and Dr. Dave Small for their advice and expertise on computations. NMR spectra were collected at the College of Chemistry NMR facility, at the University of California, Berkeley, which is supported in part by the National Institutes of Health under grant no. S10OD024998. The authors also thank Dr. Hasan Celik for advice and assistance with NMR spectroscopy and Rubber and Joy Chen as well as PMP Tech Inc. for generous gifts to our research program.

REFERENCES

(1) Pachaly, B.; Weis, J. The Direct Process to Methylchlorosilanes: Reflections on Chemistry and Process Technology. In *Organosilicon Chemistry III*; John Wiley & Sons, Ltd, 1997; pp 478−483.

(2) Seyferth, D. Dimethyldichlorosilane and the Direct Synthesis of Methylchlorosilanes. The Key to the Silicones Industry. *Organometallics* **2001**, *20*, 4978−4992.

(3) Murarka, S. P. Silicide Thin Films and Their Applications in Microelectronics. *Intermetallics* **1995**, *3*, 173−186.

(4) Schmidt, V.; Wittemann, J. V.; Senz, S.; Gösele, U. Silicon Nanowires: A Review on Aspects of Their Growth and Their Electrical Properties. *Adv. Mater.* **2009**, *21*, 2681−2702.

(5) Schmidt, V.; Wittemann, J. V.; Gösele, U. Growth, Thermodynamics, and Electrical Properties of Silicon Nanowires. *Chem. Rev.* **2010**, *110*, 361−388.

(6) De Schutter, B.; De Keyser, K.; Lavoie, C.; Detavernier, C. Texture in Thin Film Silicides and Germanides: A Review. *Appl. Phys. Rev.* **2016**, *3*, No. 031302.

(7) Ward, W. Catalysis of the Rochow Direct Process. *J. Catal.* **1986**, *100*, 240−249.

(8) Lorey, L.; Roewer, G. The Direct Synthesis of Methylchlorosilanes: New Aspects Concerning Its Mechanism. *Silicon Chem.* **2002**, *1*, 299−308.

(9) Xue, G.; Green, V. V. In *Mechanistic Aspects of the Rochow Direct Process*, Silicon for the Chemical and Solar Industry XIII; Kristiansand, Norway, 2016; pp 147−155.

(10) Sun, D.-H.; Bent, B. E.; Wright, A. P.; Naasz, B. M. Chemistry of the Direct Synthesis of Methylchlorosilanes from Methyl + Chlorine Monolayers on a Cu_3Si Surface. *Catal. Lett.* **1997**, *46*, 127−132.

(11) Lewis, K. M.; Rethwisch, D. G. *Catalyzed Direct Reactions of Silicon (Studies in Organic Chemistry)*; Elsevier: Amsterdam, 1993.

(12) Wanandi, P. W.; Glaser, P. B.; Tilley, T. D. Reactivity of an Osmium Silylene Complex toward Chlorocarbons: Promotion of Metal Redox Chemistry by a Silylene Ligand and Relevance to the Mechanism of the Direct Process. *J. Am. Chem. Soc.* **2000**, *122*, 972−973.

(13) Waterman, R.; Hayes, P. G.; Tilley, T. D. Synthetic Development and Chemical Reactivity of Transition-Metal Silylene Complexes. *Acc. Chem. Res.* **2007**, *40*, 712−719.

(14) Lipke, M. C.; Liberman-Martin, A. L.; Tilley, T. D. Electrophilic Activation of Silicon-Hydrogen Bonds in Catalytic Hydrosilations. *Angew. Chem., Int. Ed.* **2017**, *56*, 2260−2294.

(15) Hashimoto, H.; Nagata, K. Transition-Metal Complexes with Triple Bonds to Si, Ge, Sn, and Pb and Relevant Complexes. *Chem. Lett.* **2021**, *50*, 778−787.

(16) Ghana, P.; Arz, M. I.; Chakraborty, U.; Schnakenburg, G.; Filippou, A. C. Linearly Two-Coordinated Silicon: Transition Metal Complexes with the Functional Groups M≡Si—M and M = Si = M. *J. Am. Chem. Soc.* **2018**, *140*, 7187−7198.

(17) Handford, R. C.; Nguyen, T. T.; Teat, S. J.; Britt, R. D.; Tilley, T. D. Direct Transformation of SiH_4 to a Molecular $L(H)_2Co{=}Si{=}Co(H)_2L$ Silicide Complex. *J. Am. Chem. Soc.* **2023**, *145*, 3031−3039.

(18) Ghana, P.; Rump, J.; Schnakenburg, G.; Arz, M. I.; Filippou, A. C. Planar Tetracoordinated Silicon (PtSi): Room-Temperature Stable Compounds Containing Anti-van't Hoff/Le Bel Silicon. *J. Am. Chem. Soc.* **2021**, *143*, 420−432.

(19) Handford, R. C.; Smith, P. W.; Tilley, T. D. Activations of All Bonds to Silicon (Si−H, Si−C) in a Silane with Extrusion of [CoSiCo] Silicide Cores. *J. Am. Chem. Soc.* **2019**, *141*, 8769−8772.

(20) Schneider, H.; Schmidt, D.; Eichhöfer, A.; Radius, M.; Weigend, F.; Radius, U. Synthesis and Reactivity of NHC-Stabilized Iron(II)−Mesityl Complexes. *Eur. J. Inorg. Chem.* **2017**, *2017*, 2600−2616.

(21) Straus, D. A.; Zhang, C.; Quimbita, G. E.; Grumbine, S. D.; Heyn, R. H.; Tilley, T. D.; Rheingold, A. L.; Geib, S. J. Silyl and Diphenylsilylene Derivatives of $(\eta^5\text{-}C_5Me_5)(PMe_3)_2Ru$. Evidence for the Base-Free Silylene Complex $[(\eta^5\text{-}C_5Me_5)(PMe_3)_2Ru = SiPh_2]^+$. *J. Am. Chem. Soc.* **1990**, *112*, 2673−2681.

(22) Henkelman, G.; Uberuaga, B. P.; Jónsson, H. A Climbing Image Nudged Elastic Band Method for Finding Saddle Points and Minimum Energy Paths. *J. Chem. Phys.* **2000**, *113*, 9901−9904.

(23) Neumeyer, F.; Lipschutz, M. I.; Tilley, T. D. Group 8 Transition Metal Complexes of the Tripodal Triphosphino Ligands $PhSi(CH_2PR_2)_3$ (R = Ph, *i*Pr): Group 8 Transition Metal Complexes of Triphosphino Ligands. *Eur. J. Inorg. Chem.* **2013**, *2013*, 6075−6078.

(24) Schild, D. J.; Peters, J. C. Light Enhanced Fe-Mediated Nitrogen Fixation: Mechanistic Insights Regarding H_2 Elimination, HER, and NH_3 Generation. *ACS Catal.* **2019**, *9*, 4286−4295.

(25) Cavaillé, A.; Joyeux, B.; Saffon-Merceron, N.; Nebra, N.; Fustier-Boutignon, M.; Mézailles, N. Triphos−Fe Dinitrogen and Dinitrogen−Hydride Complexes: Relevance to Catalytic N_2 Reductions. *Chem. Commun.* **2018**, *54*, 11953−11956.

(26) Stone, N. J. Table of Nuclear Magnetic Dipole and Electric Quadrupole Moments. *At. Data Nucl. Data Tables* **2005**, *90*, 75−176.

(27) Ghana, P. Synthesis, Characterization and Reactivity of Ylidyne and μ-Ylido Complexes Supported by Scorpionato Ligands. Springer Theses, Springer International Publishing: Cham, 2019.

(28) Atheaux, I.; Donnadieu, B.; Rodriguez, V.; Sabo-Etienne, S.; Chaudret, B.; Hussein, K.; Barthelat, J.-C. A Unique Coordination of SiH_4: Isolation, Characterization, and Theoretical Study of $(PR_3)_2H_2Ru(SiH_4)RuH_2(PR_3)_2$. *J. Am. Chem. Soc.* **2000**, *122*, 5664−5665.

(29) Said, R. B.; Hussein, K.; Barthelat, J.-C.; Atheaux, I.; Sabo-Etienne, S.; Grellier, M.; Donnadieu, B.; Chaudret, B. Redistribution at Silicon by Ruthenium Complexes. Bonding Mode of the Bridging

Silanes in $Ru_2H_4(\mu\text{-}\eta^2{:}\eta^2{:}\eta^2{:}\eta^2\text{-}SiH_4)(PCy_3)_4$ and $Ru_2H_2(\mu\text{-}\eta^2{:}\eta^2\text{-}H_2Si(OMe)_2)_3(PCy_3)_2$. *Dalton Trans.* **2003**, 4139−4146.

(30) Reed, A. E.; Weinstock, R. B.; Weinhold, F. Natural Population Analysis. *J. Chem. Phys.* **1985**, *83*, 735−746.

(31) Parkin, G. Valence, Oxidation Number, and Formal Charge: Three Related but Fundamentally Different Concepts. *J. Chem. Educ.* **2006**, *83*, 791−799.

(32) Wolczanski, P. T. Flipping the Oxidation State Formalism: Charge Distribution in Organometallic Complexes As Reported by Carbon Monoxide. *Organometallics* **2017**, *36*, 622−631.

(33) Wiberg, K. B. Application of the Pople-Santry-Segal CNDO Method to the Cyclopropylcarbinyl and Cyclobutyl Cation and to Bicyclobutane. *Tetrahedron* **1968**, *24*, 1083−1096.

(34) Bader, R. F. W. Atoms in Molecules. *Acc. Chem. Res.* **1985**, *18*, 9−15.

(35) Handford, R. C.; Smith, P. W.; Tilley, T. D. Silylene Complexes of Late 3*d* Transition Metals Supported by *Tris*-Phosphinoborate Ligands. *Organometallics* **2018**, *37*, 4077−4085.

(36) Iluc, V. M.; Hillhouse, G. L. Arrested 1,2-Hydrogen Migration from Silicon to Nickel upon Oxidation of a Three-Coordinate Ni(I) Silyl Complex. *J. Am. Chem. Soc.* **2010**, *132*, 11890−11892.

(37) Price, J. S.; Emslie, D. J. H.; Britten, J. F. Manganese Silylene Hydride Complexes: Synthesis and Reactivity with Ethylene to Afford Silene Hydride Complexes. *Angew. Chem., Int. Ed.* **2017**, *56*, 6223−6227.

(38) Price, J. S.; Emslie, D. J. H. Interconversion and Reactivity of Manganese Silyl, Silylene, and Silene Complexes. *Chem. Sci.* **2019**, *10*, 10853−10869.

(39) The reaction of **6** with SiH_4 is described in the Supporting Information. See pages S6-S7 for additional information.

https://doi.org/10.1021/jacs.3c07998
J. Am. Chem. Soc. 2023, 145, 24690−24697